



**HAL**  
open science

## Long-wavelength Vertical-Cavity Surface-Emitting Laser using an electro-optic index modulator with 10-nm tuning range

Christophe Levallois, Bertrand Caillaud, Jean-Louis de Bougrenet de La Tocnaye, Laurent Dupont, Alain Le Corre, Hervé Folliot, Olivier Dehaese, Slimane Loualiche

### ► To cite this version:

Christophe Levallois, Bertrand Caillaud, Jean-Louis de Bougrenet de La Tocnaye, Laurent Dupont, Alain Le Corre, et al.. Long-wavelength Vertical-Cavity Surface-Emitting Laser using an electro-optic index modulator with 10-nm tuning range. *Applied Physics Letters*, 2006, 89 (1), pp.11102. 10.1063/1.2219144 . hal-00489110

**HAL Id: hal-00489110**

**<https://hal.science/hal-00489110v1>**

Submitted on 4 Jun 2010

**HAL** is a multi-disciplinary open access archive for the deposit and dissemination of scientific research documents, whether they are published or not. The documents may come from teaching and research institutions in France or abroad, or from public or private research centers.

L'archive ouverte pluridisciplinaire **HAL**, est destinée au dépôt et à la diffusion de documents scientifiques de niveau recherche, publiés ou non, émanant des établissements d'enseignement et de recherche français ou étrangers, des laboratoires publics ou privés.

# **Long-wavelength Vertical-Cavity Surface-Emitting Laser using an electro-optic index modulator with 10-nm tuning range**

**C. Levallois**

Laboratoire d'Étude des Nanostructures à Semiconducteurs, CNRS UMR Foton 6082 - INSA  
Rennes, 20 avenue des Buttes de Coësmes, 35043 Rennes Cedex, France.

**B. Caillaud, J.-L. de Bougrenet de la Tocnaye, and L. Dupont**

Optics department, CNRS UMR Foton 6082 – ENST Bretagne, CS 83818, 29238 Brest  
Cedex, France

**A. Le Corre, H. Folliot, O. Dehaese, and S. Loualiche**

Laboratoire d'Étude des Nanostructures à Semiconducteurs, CNRS UMR Foton 6082 - INSA  
Rennes, 20 avenue des Buttes de Coësmes, 35043 Rennes Cedex, France.

(Received

We demonstrate an original approach to achieving a tunable 1.55- $\mu\text{m}$  vertical-cavity surface-emitting laser. The tunability is based on an electro-optic index modulator using nano-sized droplets of liquid crystal as a phase layer. Such an approach can produce a robust and a low-cost device. A 10-nm tuning range with less than 170 V applied voltage has been demonstrated. The device is formed by a conventional InP-based active region with an epitaxial and a dielectric Bragg mirror. This optically pumped device exhibits an excellent side-mode suppression ratio of higher than 20-dB over the whole spectral range.

PACS: 42.55.Px, 42.60.Fc, 61.30.Pq

Long-wavelength vertical-cavity surface-emitting lasers (VCSELs) operating at 1.3  $\mu\text{m}$  and 1.5  $\mu\text{m}$  have been extensively studied during the last decade. Their circular and spatial single-mode beam provides very efficient fiber coupling and makes them very attractive light sources for telecommunication.<sup>1</sup> In order to increase embedded fiber communication capacities, advanced VCSELs with a tunable emission have been investigated.<sup>2</sup> These devices are suitable for wavelength division multiplexing applications in metro and local access networks. Most of the tunable VCSELs developed by researchers are comprised of an active region and an air-gap sandwiched between top and bottom distributed Bragg reflectors (DBR). The top DBR is a part of a micro-electromechanical system (MEMS) and can be moved by applying an electrostatic force which results in a change in cavity length. Electrically or optically pumped VCSELs combined with MEMS technology offer an ideal solution for wide wavelength tuning with mode-hop free emission.<sup>3,4</sup> However, this solution requires a complex processing<sup>5</sup> and is limited by their fragility. Furthermore, these mechanical systems exhibit a relatively low switching speed which depends on the MEMS structure size (few ms).<sup>2</sup> Another way to obtain a wide VCSEL bandwidth is to use a liquid crystal as an electro-optic material placed inside the cavity. The liquid crystal (LC) solution provides a large refractive index variation, but the tuning speed is less than a millisecond and it also suffers from polarization dependence due to the nematic LC birefringence. Recently, the use of nano-polymer dispersed liquid crystal (PDLC) for optical applications has shown potential for polarization independence and fast tuning speed.<sup>6,7</sup>

In this letter, we present an original use of such an electro-optic material to provide tunability of a long wavelength VCSEL. The device using a nano-PDLC material as an electro-optic index modulator is robust and easy to fabricate. The device is comprised of a conventional InP based active region, and an InP/InGaAsP bottom Bragg reflector. This half-cavity is combined with a SiO<sub>2</sub>/TiO<sub>2</sub> top dielectric Bragg reflector and the electro-optic phase

modulator in order to tune the laser emission wavelength. This optically pumped VCSEL requires less than 170V to achieve a 10 nm tunability and presents laser emission at room-temperature under pulsed-operation.

The periodic gain active region, grown by molecular beam epitaxy, has an optical length of three half-wave periods. Seven lattice-matched InGaAs/InGaAsP quantum wells (QW) are located at each antinode of the standing wave for modal gain improvement. The thicknesses of the wells and barriers are 8 nm and 10 nm, respectively. Each set is surrounded by Q<sub>1.18</sub> layers and InP layers (Q<sub>1.18</sub> is a quaternary alloy In<sub>0.8</sub>Ga<sub>0.2</sub>As<sub>0.435</sub>P<sub>0.565</sub> emitting at a wavelength of 1.18 μm). This active region is designed in order to obtain an homogenous optical absorption of the pump power and then an homogenous carrier distribution.<sup>8</sup> Prior the realization of this active region, the growth of the bottom DBR is achieved with semiconductor materials. InP and Q<sub>1.45</sub> materials (Q<sub>1.45</sub> is a quaternary alloy In<sub>0.628</sub>Ga<sub>0.372</sub>As<sub>0.8</sub>P<sub>0.2</sub> emitting at a wavelength of 1.45μm) are used as low and high refractive index, respectively. The low refractive index difference between these two materials implies the growth of 40 periods to reach a theoretical reflectivity of 99%. Following the realization of this half cavity where bottom mirror and active region are grown in a single run, a dielectric mirror is deposited on a glass substrate with an electron-beam evaporation system in order to obtain a top mirror as illustrated in Fig. 1(a). The use of dielectric materials for long wavelength VCSEL allows to obtain a high reflectivity with a small number of periods.<sup>9</sup> In our case, we use silicon dioxide and titanium dioxide material to form eight and a half pairs of TiO<sub>2</sub>/SiO<sub>2</sub> DBR on a glass substrate. The measured reflectivity for a such mirror is greater than 99.5% inside a spectral window centered around 1.55 μm. Before the realization of this dielectric DBR, a thin semi-transparent indium-thin-oxide (ITO) layer is deposited on the glass substrate in order to apply the electric field on the phase layer. The second electrode

consists in a 200 nm gold layer on the back of the InP substrate. The InP substrate and the epitaxial layers are N-doped. Consequently, the major part of the electric field is applied on the nano-PDLC phase layer and the dielectric DBR.

Fig. 1(a) illustrates the last processing stage, where the half cavity and the top mirror are joined together thanks to micrometric spacers in order to obtain an air gap of 6  $\mu\text{m}$  with an accuracy to within 2%. The phase layer, which is comprised of a suspension of nematic LC (BL 24 from Merck) and a ultraviolet (UV) curable monomer (NOA 81 from Norland) is introduced between the dielectric Bragg mirror and the active region. The mixture, with a LC ratio of 30% in weight, is irradiated through the top mirror with strong UV light ( $\lambda = 365 \text{ nm} - 350 \text{ mW/cm}^2$ ) in order to realize the photopolymerization-induced phase separation (PIPS).<sup>10</sup> Finally, the index modulator layer, whose refractive index is close to  $n = 1.55$ , has an optical length of  $6\lambda$ , and can be used to obtain an isotropic refractive index variation for the plane which is perpendicular to the applied electric field. The applied bias voltage orients the LC droplets with respect to the induced electric field and hence creates a refractive index decrease. The refractive index variation is maximum when almost all of the LC droplets are oriented along the field direction. Fig. 1(b) illustrates the squared modulus of the intra-cavity stationary electrical field. The active and tuning layer thicknesses (0.7  $\mu\text{m}$  and 6  $\mu\text{m}$  respectively) were chosen in order to reach high enough gain for laser emission and a relatively large tuning range. A large fraction of the intensity is thus located in the nano-PDLC layer. Consequently nano-PDLC absorption must be low. The major contribution for these losses is related to the scattering of light by the LC droplets. However, for our LC droplets, the expected size is close to 100 nm and the absorption is minimized. Optical losses close to  $15 \text{ cm}^{-1}$  at 1.55  $\mu\text{m}$  have been measured for samples comprising a nano-PDLC layer sandwiched between two glass substrate. These optical losses are observed when LC droplets are randomly oriented without electric field and they are reduced when an electric field is

applied. The switching time also depends on the size of the LC droplets, and it decreases as the droplet size is reduced.<sup>11</sup> However, the electrical field needed to switch LC droplets increases. Thus, the size of LC droplets is a crucial parameter which can be controlled by the UV power during PIPS process.<sup>11</sup>

The fabricated VCSEL have been optically pumped in order to achieve lasing emission. The optical pumping experiment consists of focusing a pulsed laser beam ( $\lambda = 1.064 \mu\text{m}$ ) with a microscope objective on the dielectric DBR. The constant pulse width is 1 ns with a repetition rate of 6.6 kHz. The photopumped spot is circular with an area of  $200 \mu\text{m}^2$ , and the laser emission is collected back with the same objective and transmitted through a beam splitter and a filter. The signal is injected in a large core diameter optical fiber connected to a spectrum analyzer. Fig. 2 shows emission spectra under constant optical pumping at different tuning voltage values. As the applied voltage between the top and bottom DBRs is increased from 0 to 170 V, the VCSEL wavelength is tuned from 1561.6 to 1551.8 nm. The increase of the applied voltage on the VCSEL reduces the refractive index of the nano-PDLC layer and therefore shifts the laser emission to shorter wavelengths. A tuning range of 9.8 nm is then demonstrated with an applied voltage close to 170V. All the spectra presented in Fig. 2 have been recorded for a pump power level equal to one and a half times the threshold pump power value at 0V. For no applied electric field, the threshold power density has been estimated at  $30 \text{ kW}\cdot\text{cm}^{-2}$  and this value will be discussed afterwards. As illustrated in Fig.2, the side-mode suppression ratio is in excess of 20 dB for the whole tuning range. The peak power emitted by the VCSEL at 0V, for the pump power used to record the lasing spectra, is 2.1 mW. The free spectral range (FSR) has been estimated using a transfer matrix formalism based on our VCSEL structure. The calculated FSR is larger than 50 nm which is highly compatible with the observed tuning range of 10 nm. Consequently, the FSR is sufficient to eliminate mode hopping during wavelength tuning. In addition, the two nearest

optical modes are outside of the narrow spectral bandwidth of the InP/InGaAsP bottom mirror. Thus, only a single wavelength emission can be obtained and tuned.

The Fig. 3 depicts the wavelength tunable range as a function of the voltage applied on the VCSEL structure. The wavelength decreases with a sigmoid behaviour when voltage increases and approaches saturation at around 150V. The tunability efficiency is maximum in the middle of the sigmoid curve, close to 90V, and reaches 0.16 nm/V. The saturation tendency which occurs at high voltage means that the LC droplets become almost completely aligned in the direction of the electric field and the maximum index variation is reached. This index variation is given by the following expression:<sup>12</sup>  $\Delta n_{max} = X_{CL} \cdot \eta \cdot \delta n / 3$ , where  $X_{CL}$  is the fraction of LC in the polymer,  $\delta n$ , equal to 0.2, is the birefringence of the LC, and  $\eta$  the factor which takes into account the effective part of LC which can participate in the refractive index change. In our case, the tuning range of 10 nm corresponds to a refractive index variation of  $\Delta n_{max} = 1.5 \cdot 10^{-2}$ . This suggests that the efficient fraction of LC droplets in the polymer matrix ( $X_{CL} \cdot \eta$ ) which can contribute to the index change is about 20%.

The solid line curve plotted in Fig. 3 shows the laser peak wavelength calculated from the quadratic dependency of the refractive index with the electric field. In agreement with a previous work,<sup>6</sup> the simulation based on the transfer matrix formalism and this relationship provide a good approximation of the wavelength shift in the weak electrical field limit. As illustrated in Fig. 3, for a constant pump power, the VCSEL output power depends on the applied electric field. As the applied voltage between the top and bottom DBR is increased from 0 to 170V, the VCSEL output power increases by 3 dB. However, the simulated modal gain given by the following expression:  $g_{mod} = \Gamma \cdot g_{mat}$ , where  $g_{mat}$  is the material gain for the used QWs and  $\Gamma$  is the spatial overlap factor, remains constant for a spectral range of 10 nm around 1.55  $\mu\text{m}$ . Now, we consider the net gain:  $g_{net} = g_{mod} - \alpha$ , where  $\alpha$  is the average loss coefficient per unit length in the cavity taking account losses in the

semiconductor, nano-PDLC and through the mirrors. The losses through the mirrors and semiconductor materials are also approximately constant within the tunable spectral window. Thus, this variation of the emitted power can be explained by the decrease of losses related to LC droplets scattering during the wavelength tuning. When LC droplets are randomly oriented, the scattering losses inside the phase layer are higher than when the voltage is maximum and almost of the LC droplets are aligned with the applied electric field.

Consequently, the pump power threshold is higher when all the LC droplets are randomly oriented without voltage applied on the VCSEL. As previously stated, for no applied voltage, this power is close to  $30 \text{ kW}\cdot\text{cm}^{-2}$ . This threshold value is high but it can be explained by optical losses which are higher than expected. As mentioned above, the UV power used during PIPS process is a crucial parameter. In our case, a part of the incident UV power is absorbed by the  $\text{SiO}_2/\text{TiO}_2$  dielectric Bragg mirror. Consequently the size of the LC droplets is probably larger than 100 nm which implies optical losses higher than  $15 \text{ cm}^{-1}$ . A spin-coated method is under study to improve the UV irradiation of the polymer in order to obtain smaller optical losses for the electro-optic layer.<sup>6</sup> Others optimizations can be carried out like the use of a more efficient semiconductor DBR for the bottom mirror. Larger tuning ranges could be obtained with larger birefringence LCs<sup>13</sup> or higher concentration of LC droplets. For practical use, the main limiting factor is the driving voltage. However, this voltage can be reduced by introducing thin ITO electrodes with a low optical absorption inside the cavity, close to the nano-PDLC layer to avoid the voltage drop induced by the dielectric DBR.

In conclusion, a VCSEL with an electro-optic material inside the cavity shows a laser emission with a 10 nm tuning range around  $1.55 \mu\text{m}$  wavelength under 170V applied voltage. The device is easy to realize and does not need complex processing as in MEMS VCSEL. The



switching times are expected to be about a hundred  $\mu\text{s}$ . The use of a more efficient bottom DBR and smaller LC droplets will improve pump power near the threshold in order to develop an electrically pumped VCSEL. Finally, the high voltage value can be reduced by employing and introducing ITO electrodes with low optical losses inside the cavity, close to the nano-PDLC layer.

### **Acknowledgments**

The authors wish to thank the Brittany region for supporting this project and the Kerdry company for manufacturing the dielectric Bragg mirrors.

## References

1. A. Karim, J. Piprek, P. Abraham, D. Lofgreen, Y.-J. Chiu, and J. E. Bowers, *IEEE J. Select. Topics in Quantum Electron.* **7**, 1244 (2001).
2. C.J. Chang-Hasnain, *IEEE J. Select. Topics in Quantum Electron.* **6**, 978 (2000).
3. F. Riemenschneider, M. Maute, H. Halbritter, G. Boehm, M.-C. Amann, and P. Meissner, *IEEE Photon. Technol. Lett.* **16**, 2212 (2004).
4. D. Vakhshoori, P. Tayebati, C.C. Lu, M. Azimi, P. Wang, J.H. Zhou and E. Canoglu, *Electron. Lett.* **35**, 900 (1999).
5. D. Sun, W. Fan, P. Kner, J. Boucart, T. Kageyama, D. Zhang, R. Pathak, R.F. Nabiev, and W. Yuen, *IEEE Photon. Technol. Lett.* **16**, 714 (2004).
6. S. Matsumoto, K. Hirabayashi, S. Sakata, and T. Hayashi, *IEEE Photon. Technol. Lett.* **11**, 442 (1999).
7. H. Ren, Y.-H. Fan, Y.-H. Lin, S.-T. Wu, *Optics Communications* **247**, 101 (2005).
8. J. Geske, K. G. Gan, Y. L. Okuno, J. Piprek, and J. E. Bowers, *IEEE J. Quantum Electron.* **40**, 1155 (2004).
9. J. Kinoshita, T. Miyamoto, Y. Onishi, and Fumio Koyama, *Jpn. J. Appl. Phys.* **43**, 5928 (2004).
10. L. Bouteiller and P. Le Barny, *Liquid. Cryst.* **21**, 157 (1996).
11. H. Ren and S.-T. Wu, *Appl. Phys. Lett.* **81**, 3537 (2002).
12. V. Verbrugge, J.-L. de Bougrenet de la Tocnaye, and L. Dupont, *Optics Communication* **215**, 353 (2003).
13. C. Sekine, N. Konya, M. Minai, K. Fujisawa, *Liquid Cryst.*, **28**, 1495 (2001).

## Figures captions

### Figure 1

(Color online). Schematic of the cross-section of the tunable nano-PDLC VCSEL (a). Modulus squared of the stationary electric field intensity in the structure layers with no applied voltage on VCSEL (b).

### Figure 2

(Color online). Emission spectra at different tuning voltage values for a constant pump power ( $P_{pump} = 1.5 \cdot P_{th}$  at 0V). Tuning voltage values are indicated above each peak, in volts .

### Figure 3

Emission wavelength and output power of the VCSEL as function of the applied voltage. The solid curve is the simulated wavelength variation for low tuning voltage.

FIG. 1.

C. Levallois *et al*

Applied Physics Letters

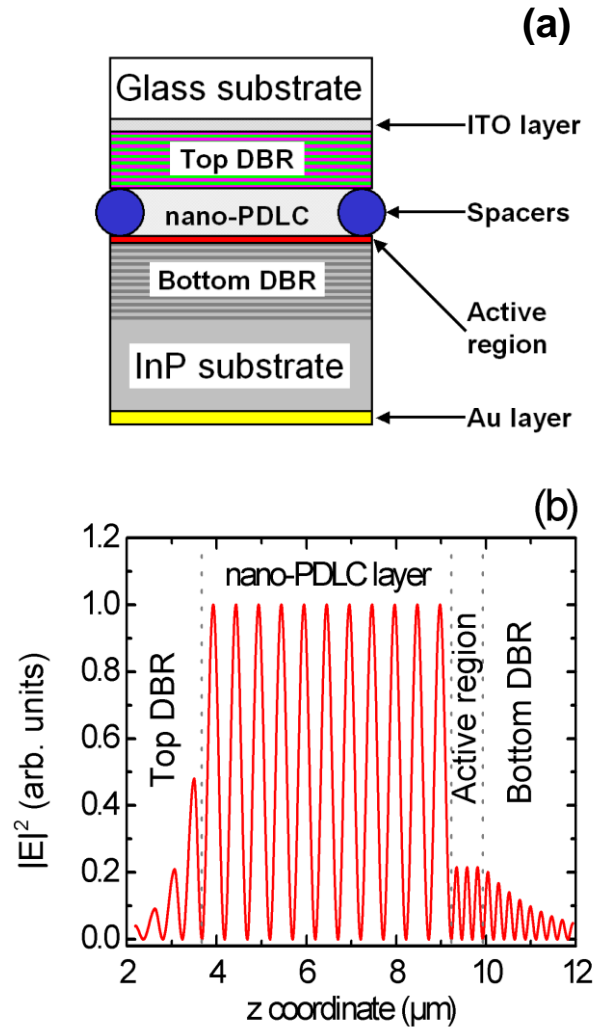


**FIG. 2.**

C. Levallois *et al*

Applied Physics Letters

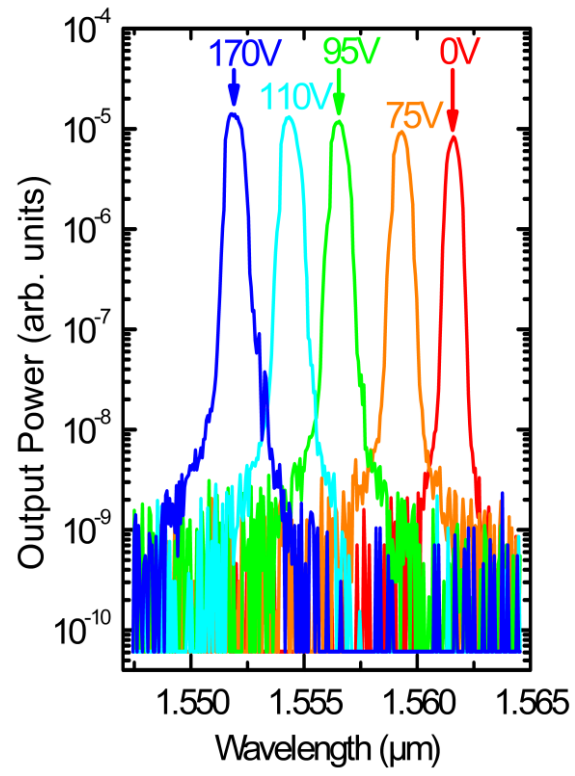


FIG. 3.

C. Levallois *et al*

Applied Physics Letters

